Oceanologia (2017) 59, 365—378

Available online at www.sciencedirect.com

ScienceDirect

journal homepage: www.journals.elsevier.com/oceanologia/

ORIGINAL RESEARCH ARTICLE

The relationship between Suspended Particulate Matter and Turbidity at a mooring station in a coastal environment: consequences for satellite-derived products

Madihah Jafar-Sidik [a,b,*], Francis Gohin [c,], David Bowers [b], John Howarth [d], Tom Hull [e]**

[a] *Borneo Marine Research Institute, Universiti Malaysia Sabah, Kota Kinabalu, Malaysia*
[b] *School of Ocean Sciences, Bangor University, Anglesey, United Kingdom*
[c] *Ifremer, Dyneco/Pelagos, Centre Ifremer de Brest, Plouzane, France*
[d] *National Oceanography Centre, Joseph Proudman Building, Liverpool, United Kingdom*
[e] *Centre for Environment, Fisheries and Aquaculture Science (Cefas), Lowestoft, United Kingdom*

Received 3 February 2017; accepted 7 April 2017
Available online 26 April 2017

KEYWORDS
Turbidity;
Suspended matter;
MODIS;
Irish Sea

Summary From a data set of observations of Suspended Particulate Matter (SPM) concentration, Turbidity in Formazin Turbidity Unit (FTU) and fluorescence-derived chlorophyll-*a* at a mooring station in Liverpool Bay, in the Irish Sea, we investigate the seasonal variation of the SPM: Turbidity ratio. This ratio changes from a value of around 1 in winter (minimum in January—February) to 2 in summer (maximum in May—June). This seasonal change can be understood in terms of the cycle of turbulence and of the phytoplankton population that affects the nature, shape and size of the particles responsible for the Turbidity. The data suggest a direct effect of

* Corresponding author at: Borneo Marine Research Institute, Universiti Malaysia Sabah, 88450 Kota Kinabalu, Sabah, Malaysia. Tel.: +60 88320000x2600; fax: +60 88320261.
** Corresponding author at: Ifremer, Dyneco/Pelagos, Centre Ifremer de Brest, BP 70, F-29280 Plouzane, Brittany, France. Tel.: +33 298224315; fax: +33 298224548.
E-mail addresses: madihahjsm@gmail.com (M. Jafar-Sidik), Francis.Gohin@ifremer.fr (F. Gohin), d.g.bowers@bangor.ac.uk (D. Bowers), mjh@noc.ac.uk (J. Howarth), tom.hull@cefas.co.uk (T. Hull).
Peer review under the responsibility of Institute of Oceanology of the Polish Academy of Sciences.

Production and hosting by Elsevier

http://dx.doi.org/10.1016/j.oceano.2017.04.003

phytoplankton on the SPM:Turbidity ratio during the spring bloom occurring in April and May and a delayed effect, likely due to aggregation of particles, in July and August. Based on the hypothesis that only SPM concentration varies, but not the mass-specific backscattering coefficient of particles b_{bp}^*, semi-analytical algorithms aiming at retrieving SPM from satellite radiance ignore the seasonal variability of b_{bp}^* which is likely to be inversely correlated to the SPM:Turbidity ratio. A simple sinusoidal modulation of the relationship between Turbidity and SPM with time helps to correct this effect at the location of the mooring. Without applying a seasonal modulation to b_{bp}^*, there is an underestimation of SPM in summer by the Ifremer semi-analytical algorithm (Gohin et al., 2015) we tested. SPM derived from this algorithm, as expected from any semi-analytical algorithm, appears to be more related to in situ Turbidity than to in situ SPM throughout the year.

1. Introduction

Suspended Particulate Matter (SPM) is a major component of the coastal environment that is monitored for multiple purposes. We may name among them a better knowledge of sediment transport and the response of the suspended sediment load to resuspension, deposition, and river discharge. Through light absorption and scattering the SPM also contributes to water clarity and governs the amount of photons available for photosynthesis in the water column. Suspended matter is also a state variable of the sediment transport and biogeochemical models of coastal seas. The geographical distribution of SPM concentration is key for analyzing the deposition and erosion patterns in an estuary and evaluating the material fluxes from river to sea. Satellite remote-sensing, associated with instrumented moorings, provide useful data for investigating the spatial and temporal variation of SPM in estuarial and coastal zones. Some of these algorithms (Binding et al., 2003; Forget et al., 1999; Lahet et al., 2000; Li et al., 1998) are empirical and others (Eleveld et al., 2008; Gohin et al., 2005; Han et al., 2016; Nechad et al., 2010; Van der Woerd and Pasterkamp, 2008) are semi-analytical as they make use of the Inherent Optical Properties (IOPs) of the water constituents. Products of non-algal SPM derived from the Ifremer semi-analytical algorithm (Gohin et al., 2005; Gohin, 2011) have been provided for years to a large community and used, with or without in situ data, for validating hydro-sedimentary models (Edwards et al., 2012; Ford et al., 2017; Guillou et al., 2015, 2016; Ménésguen and Gohin, 2006; Sykes and Barciela, 2012; Van der Molen et al., 2016, 2017) or forcing the light component in biogeochemical modelling (Huret et al., 2007) over the northwest European continental shelf.

Autonomous observation platforms such as ferrybox or instrumented buoys typically do not provide SPM concentration directly but instead provide Turbidity measurements. Turbidity data are by far the most frequent data set related to SPM provided to the scientific community and managers of the coastal environment. For this reason and as Turbidity is tightly related to backscattering, Dogliotti et al. (2015) suggest making use of a semi-analytical relation to estimate Turbidity from marine reflectance and, in a second step, derive SPM from Turbidity. All semi-analytical methods aiming to retrieve directly SPM concentration assume the stability of the mass-specific backscattering, b_{bp}^*, which is considered as constant in space and throughout the seasons. This assumption remains to be verified in coastal waters where there is a seasonal variation in the nature of the SPM, from small mineral particles in winter to phytoplankton cells, aggregates and flocs in summer.

Martinez-Vicente et al. (2010) observed a seasonal effect on the scattering properties of particles at a coastal station of the Western English Channel (the L4 station located off Plymouth at 50.25N, 4.22W). These authors observed that the SPM:b_p(555) ratio (where b_p is the scattering coefficient of mineral and organic particles) varies between a winter mean of 2 and a summer mean of 1.1 g m^{-2}. The mean mass-specific particle backscattering coefficient, b_{bp}^* was 0.0027 m^2 g^{-1} for total SPM at 532 nm, and higher with respect to Suspended Particulate Inorganic Matter (SPIM). The measured mass-specific backscattering, b_{bp}^*, was 0.0075 in winter and 0.0023 m^2 g^{-1} in summer; which is at the lower end of values reported for coastal waters (Berthon et al., 2007; Snyder et al., 2008). Given the small amount of data available, however, the authors recognised that it was difficult to draw conclusions about the seasonality of this coefficient. At the L4 station, the SPM mean value was relatively low for a coastal site (1.00 ± 0.88 g m^{-3}) with peaks in winter (with a stronger contribution of SPIM). However, the highest winter peak of 9.94 g m^{-3} is lower than that observed in general in coastal waters (up to 100 g m^{-3} in winter). A particularly high content of mineral particles in winter and strong phytoplankton blooms in summer are likely to emphasise the variability of the inorganic:organic fraction for suspended particles in coastal waters with consequences for the backscattering properties.

In a study encompassing a large range of water types, Neukermans et al. (2012) observed that waters dominated by mineral particles backscatter up to 2.4 times more per unit mass, $b_{bp}^* = 0.0121$ m^2 g^{-1}, than waters dominated by organic particles, $b_{bp}^* = 0.0051$ m^2 g^{-1} at 650 nm. Similar conclusions were pointed out in Arctic seawaters by Reynolds et al. (2016) who observed that the average b_{bp}^* of mineral assemblages was almost twice that of organic assemblages. The positive dependency of the mass-specific backscattering coefficient on the SPIM:SPM ratio has also been shown by Bowers et al. (2014).

In the Irish Sea, McKee and Cunningham (2006) identified two water sub-types that are distinguished both optically and by the ratio of the concentrations of their constituents (Chl:SPIM). The Inherent Optical Properties (IOPs) at stations with a low ratio of chlorophyll-*a* to suspended particles, Group "Mineral", were highly correlated with the concentration of

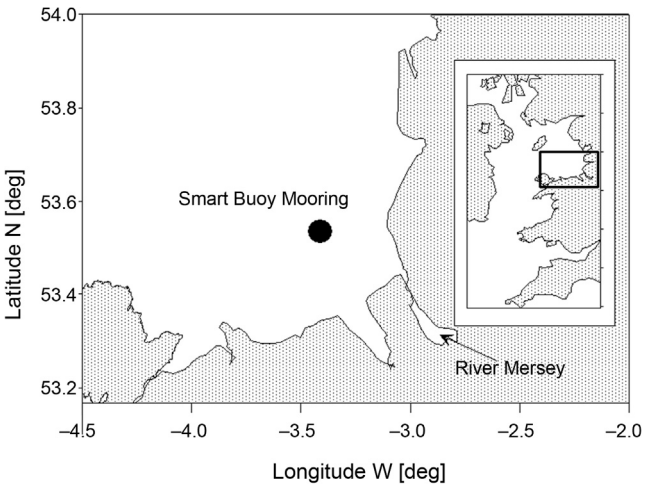

Figure 1 Location of the Cefas SmartBuoy at the Liverpool Bay coastal observatory in the Irish Sea.

SPIM, while those for Group "Phytoplankton" were largely determined by Chlorophyll concentration. At the "Mineral" stations, b_{bp}^*, relative to SPIM, was 0.014 $m^2\ g^{-1}$ at 676 nm. For modelling the reflectance of the Irish Sea waters, Neil et al. (2011) proposed 0.015 and 0.014 $m^2\ g^{-1}$ for b_{bp}^*, relative to mineral SPM, at 555 and 667 nm respectively.

Using a large data set of Turbidity, fluorescence and SPM observations acquired at the Cefas SmartBuoy of the Liverpool Bay coastal observatory in the Irish Sea (Fig. 1), we investigate the seasonal cycle of Turbidity, SPM and Chlorophyll during several years (2003–2010). The yearly cycle of the SPM:Turbidity ratio is expected to be closely related to that of the SPM:b_{bp} ratio. To this purpose we consider the backscattering coefficient of particles *bbp* derived from a semi-analytical algorithm for SPM from MODIS radiance (Gohin et al., 2005; Gohin, 2011). Although this semi-analytical algorithm has been designed for estimating SPM directly without any calibration of *bbp*, which is only an intermediate parameter, this latter quantity appears in the algorithm in the green and red bands for low and high turbidity respectively. We will investigate the relationship between satellite-derived *bbp*, turbidity, and SPM. The need for using a seasonally-varying mass-specific backscattering coefficient in remote sensing algorithms for SPM in coastal waters can then be assessed.

2. Data and methods

2.1. In situ data

The area studied in this work is Liverpool Bay in the eastern Irish Sea (Fig. 1). Liverpool Bay is shallow (typical depths less than 30 m) and has a large tidal range, up to 9 m at the coast. There is a significant input of freshwater from the Mersey and other rivers, mainly along the eastern side of the bay. The freshwater input can produce intermittent stratification in the bay at all times of year and particularly at neap tides and times of low wind (Sharples and Simpson, 1995). At the Liverpool Bay mooring, and more generally in most of UK coastal waters, Devlin et al. (2009) observed that the diffuse attenuation coefficient (K_D) is driven by SPM more than Chlorophyll or Chromophoric Dissolved Organic Matter (CDOM); hence the importance of SPM for understanding the seasonal variability of the water transparency in Liverpool Bay.

Turbidity data are obtained from a time-series of measurements at a SmartBuoy mooring in the bay. The buoy, located at 53.53N and 3.36W, was deployed in August 2002, operated as part of the Coastal Observatory run by the National Oceanography Centre, Liverpool. Turbidity is measured using a Seapoint auto-ranging Optical Backscatter Sensor turbidimeter (OBS, Seapoint USA Inc.). The OBS sensor measures infra-red radiation (880 nm) scattered by particles in the water at angles ranging from 140° to 165°. The resulting Turbidity measurements are expressed in Formazin Turbidity Units (FTU). The OBS sensor collected continuous Turbidity data at 30 min intervals between 1 and 2 m below the water surface (Mills et al., 2005). SPM measurements are also carried out at the SmartBuoy using water samples collected automatically, every 24 h at midnight, by an Aqua Monitor (WMS-2 Aqua Monitor, Envirotech Inc., USA). The 150 ml samples of sea water collected by the Aqua Monitor were sent to a laboratory for analysis by filtration to provide SPM concentration (in g m^{-3}).

The samples were filtered using pre-weighed Cyclopore 0.4 μm polycarbonate filters, rinsed and desiccated under vacuum until constant weight was obtained (Loring and Rantala, 1992). In total, there are 1246 water samples collected by the automatic water sampler over the 8-year study period (2003–2010). From samples of 2000 ml of sea water obtained during regular cruises by the research vessel Prince Madog, 73 additional SPM measurements were also available, giving a total of 1319 samples of SPM at the mooring for the 2003–2010 period.

Chlorophyll concentration was obtained from in situ fluorescence measurements (expressed in arbitrary units) measured by a Seapoint SCF fluorometer. GF/F filtered samples, taken during deployment and recovery of the instruments, were analysed for chlorophyll-*a* using a phaeopigment corrected (acidified) fluorometric method (Tett, 1987). These samples were used for calibrating the fluorescence measurements to chlorophyll-*a*.

The turbidimeter and the fluorometer were located at a depth of 1–2 m below the surface and data are recorded using the Cefas ESM2 data-logger configured for a 10 min measuring burst every 30 min, with the sensors sampling at 1 Hz. Two identical sets of instruments are used and the mooring is replaced every 3–6 weeks.

2.2. Satellite data and algorithm

Data from the MODIS-Aqua sensor corresponding to the period 2003–2010 have been used. These remote-sensing reflectance products (Level 2) have been provided by the Ocean Color NASA/GSFC Centre after the 2012 reprocessing of the archive. Data are projected onto a regular grid of 1.2 × 1.2 km. The standard NASA CLOUD flag is applied. A uniformity test, based on the deviation of the pixel Chlorophyll-*a* to the local mean, was then applied to eliminate pixels close to cloud-flagged areas.

The semi-analytical model used to retrieve non-algal SPM from satellite reflectance is described in Gohin et al. (2005) and Gohin (2011). Non-algal SPM (NA_SPM), defined as non-living SPM (not related to Chl) in the 2005 publication, is estimated from radiance at 555 nm and 667 nm after a preliminary estimation of the chlorophyll-*a* concentration by the OC5 algorithm (Gohin et al., 2002; Tilstone et al., 2017). Depending on the NA_SPM level retrieved, the final NA_SPM is chosen at 555 nm if NA_SPM at 555 nm is less than 4 g m^{-3} and NA_SPM at 667 nm less than 3.9 g m^{-3}. This is generally the case in relatively clear waters. In other cases NA_SPM (670) is chosen.

The semi-analytical algorithm proceeds in two steps for estimating NA_SPM at 555 nm and 667 nm. In the first step an intermediate term R′ is estimated from the normalised water-leaving radiance nLw. The normalised water-leaving radiance, is the light that would exit the ocean with a sun at the zenith in the absence of an atmosphere and at the mean earth-sun distance. It is obtained by multiplying the remote-sensing reflectance by the extraterrestrial solar irradiance provided by NASA for each MODIS-Aqua waveband.

$$R' = \alpha_0 + \alpha_1 nLw, \tag{1}$$

here α_0 and α_1 are two constants defined for each wavelength (551 and 667 nm).

R' is related to the backscattering and absorption coefficients by

$$R' = \frac{b_b}{a + b_b}. \tag{2}$$

In Eq. (2), a and b_b are the absorption and backscattering coefficients (wavelength-dependent). These coefficients can be written in terms of the concentration of Chl and SPM as shown in Eq. (3).

$$\begin{aligned} a &= a_w + a^*_{\mathrm{chl}} \times \mathrm{Chl} + a^*_{\mathrm{nap}} \times \mathrm{NA\_SPM}, \\ b_b &= b_{bw} + b^*_{b\mathrm{Chl}} \times \mathrm{Chl} + b^*_{\mathrm{bnap}} \times \mathrm{NA\_SPM}, \end{aligned} \tag{3}$$

where the * quantities represent the mass-specific IOPs (of Chl and NA_SPM); w indicates pure water. A specific contribution of coloured dissolved organic material (CDOM) to absorption in these green and red wavelengths is ignored in the algorithm. Absorption by CDOM associated with the decay of phytoplankton is accounted for through $a_{\mathrm{Chl}}{}^*$.

After making these substitutions, the NA_SPM concentration is then obtained by inverting Eq. (2):

$$\mathrm{NA\_SPM} = \frac{R' x [a_w + b_w + (a^*_{\mathrm{chl}} + b^*_{b\mathrm{Chl}}) \times \mathrm{Chl}] - [b_{\mathrm{bw}} + b^*_{b\mathrm{Chl}} \mathrm{Chl}]}{b^*_{\mathrm{bnap}} - (a^*_{\mathrm{nap}} + b^*_{\mathrm{bnap}}) \times R'}. \tag{4}$$

The constants α_0 and α_1 of Eq. (1) have been obtained by minimisation of the variance of the errors derived from Eq. (4) applied to a data set of coastal SPM and satellite reflectance (see Gohin et al., 2005 for details). These constants calculated for North West European waters are presented in Table 1.

The specific backscattering coefficients, $b_{\mathrm{bnap}}{}^*(555)$ and $b_{\mathrm{bnap}}{}^*(667)$ have been set from the literature to 0.0074 and 0.0058 $m^2\ g^{-1}$ respectively (Gohin et al., 2005; Gohin, 2011). These values are similar to those proposed by Martinez-Vicente et al. (2010) for the L4 station in the English Channel but lower than those proposed (relative to SPIM) by McKee and Cunningham (2006) for the Irish Sea and Neukermans et al. (2012) for different coastal waters. However, $b_{\mathrm{bnap}}{}^*(555)$ is compatible with $b_{\mathrm{bp}}{}^*(555)$ found by Woźniak (2014) for the southern Baltic Sea ($0.0065 \pm 0.0030\ m^2\ g^{-1}$).

The algal SPM, A_SPM, has been approximated in Gohin et al. (2005) by Eq. (5) taken from Morel (1988):

$$\mathrm{A\_SPM} = 0.234 \times \mathrm{Chl}^{0.57} \text{ for Chl in } [\mathrm{mg\ m^{-3}}] \text{ and SPM in } [\mathrm{g\ m^{-3}}]. \tag{5}$$

This formula can be applied to both in situ and satellite Chlorophyll-*a* for providing an estimation of the SPM originating from the bloom itself.

3. Results and discussion

3.1. The seasonal cycle of non-algal SPM and Chlorophyll-*a* observed from space and in situ at the location of the buoy

By application of the semi-analytical algorithm, we obtain the seasonal dynamics of non-algal SPM (Fig. 2) and Chlorophyll-*a* (Fig. 3) throughout the seasons in the vicinity of the station. The results are presented as monthly averages. We see in Fig. 2 that the buoy is located on the margin of a high turbidity area. The seasonal variation of non-algal SPM can be related to large waves from October to March with a maximum in January (Wolf et al., 2011).

Fig. 4 shows monthly-averaged satellite-derived non-algal SPM and Chlorophyll-*a* at the SmartBuoy. The number of data points in each month ranges from 22 in December to 63 in June (Table 2). Satellite-derived Chlorophyll-*a* in the winter months is likely to be overestimated. Although the satellite algorithm is developed for this type of waters (calibrated on the English Channel, Bay of Biscay and the coastal waters of the Northwest Mediterranean Sea), yellow substances, SPM and low solar zenith angles could affect the estimation significantly in the Irish Sea.

Monthly averaged satellite non-algal SPM and Chl-*a* (Fig. 4) show patterns similar to those obtained in situ (Fig. 5). In Fig. 5, SPM and Turbidity are well related but Turbidity in summer appears to be particularly low relative to SPM.

Table 1 α_0 and α_1, relating the MODIS-Aqua normalised water-leaving radiance to R' (Eq. (1)), and $b_{\mathrm{bnap}}{}^*$ in the NA_SPM algorithm. α_0 and α_1 have been obtained by minimisation and $b_{\mathrm{bnap}}{}^*$ are set from the literature.

	α_0 [m W^{-1} cm^2 str μm]	α_1 [m W^{-1} cm^2 str μm]	$b_{\mathrm{bnap}}{}^*$ [$m^2\ g^{-1}$]
Green wavelength (555 nm)	0.03	0.032	0.0074
Red wavelength (667 nm)	0.06	0.04	0.0058

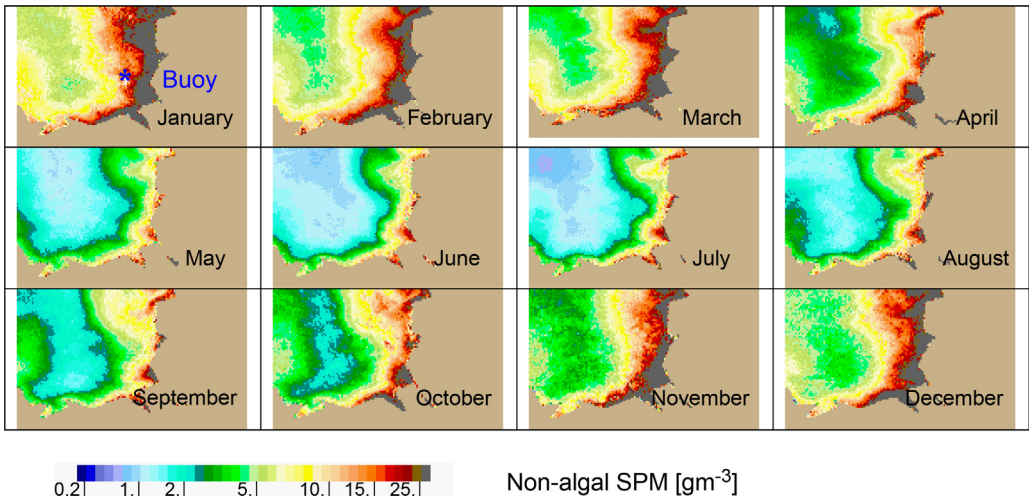

Figure 2 Satellite composites of monthly-averaged concentration of non-algal SPM for the period 2003–2010 (the area covered in these figures corresponds to the rectangle shown in Fig. 1). The location of the buoy is indicated on the image of January.

3.2. Turbidity, SPM and Chlorophyll-*a* observed in situ

Monthly-averaged concentrations of in situ SPM and satellite-derived SPM with the proportion of algal and non-algal components are presented in Fig. 6a Agreement between satellite and in situ SPM is good but satellite-derived SPM appears to be lower than in situ SPM from May to October. This was also observed by Van der Molen et al. (2017). The fraction of algal SPM in the total SPM retrieved from satellite reflectance (Fig. 6b) is relatively low except in May and during the productive season.

Fig. 7 shows plots of in situ SPM versus Turbidity in two-month blocks. The slope of the regression of SPM versus Turbidity forced through the origin ranges from 0.9 g m^{-3} FTU^{-1} in winter, when mineral particles are dominant, to 1.5 g m^{-3} FTU^{-1} in May–June when phytoplankton contribution to the overall IOPs of the medium is expected to be the highest (see Table 3). The determination coefficients (R^2) are the lowest in summer. The coefficient of determination is negative in May–June (Fig. 7c); which means that a simple mean is better than a regression forced through the origin. In fact, these ratios follow a continuous evolution that we can represent with a cosine function.

The seasonal variability of SPM related to Turbidity and Chl-*a* (and derived algal SPM) will be expressed through Eq. (6).

$$\mathrm{SPM} = \left[\alpha + \beta \times \left(1 - \cos\left(\frac{\mathrm{time} \times 2\pi}{365}\right)\right)\right] \times [\mathrm{Turbidity} - \chi \times \mathrm{algal\ SPM}] + \mathrm{algal\ SPM}, \quad (6)$$

where time is the day of the year and SPM is total SPM. Turbidity is in FTU.

The term α, in [g m^{-3} FTU^{-1}], is the SPM:Turbidity ratio at the beginning of the year when the phytoplankton biomass is low and SPM is dominated by SPIM. It is also the minimum value reached by this ratio. β is the amplitude of the seasonal variation of the ratio. χ, in [FTU g^{-1} m^{-3}], is the Turbidity: SPM ratio for phytoplankton and related particles.

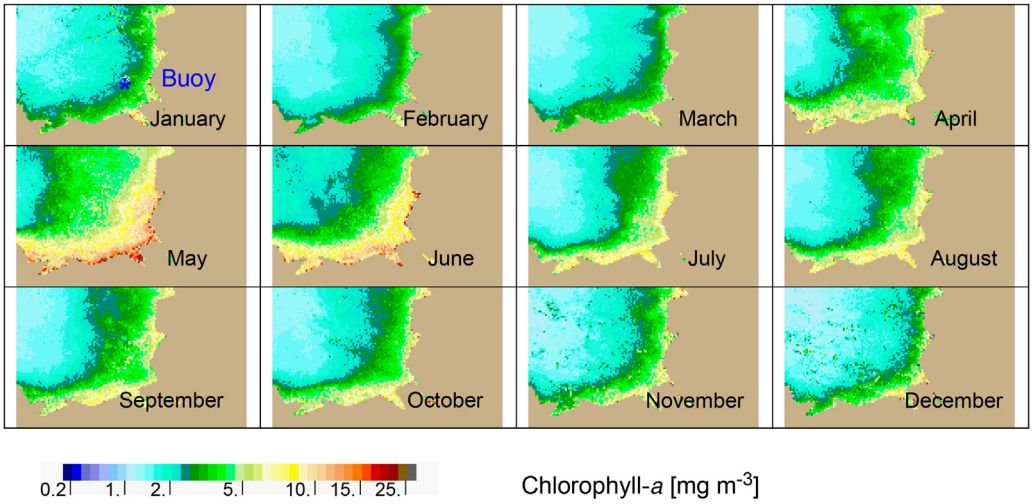

Figure 3 Satellite composites of monthly-averaged concentration of Chlorophyll-*a* for the period 2003–2010 (the area covered in these figures corresponds to the rectangle shown in Fig. 1).

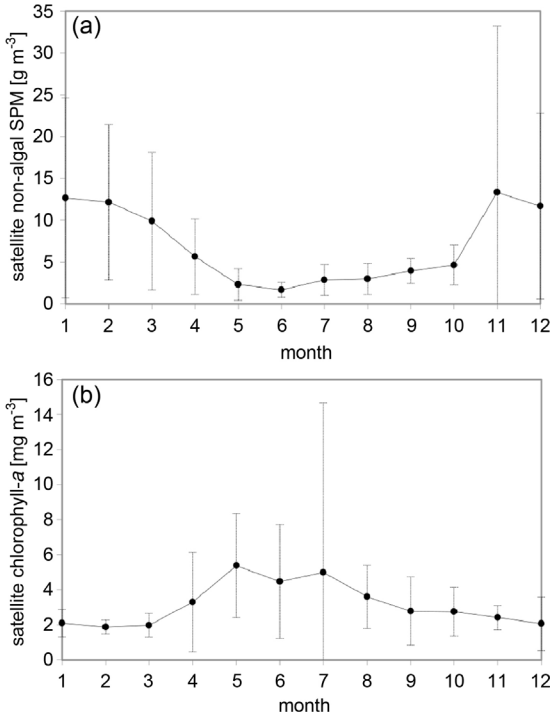

Figure 4 Monthly-averaged concentration of satellite-derived non-algal SPM and Chlorophyll-*a* at the mooring site. Bars indicate ± one standard deviation about the mean.

The seasonal variation is modelled here with only one harmonic. Other harmonics could be added if sufficient data were available as the role of phytoplankton on the ratio could reach a first peak during the spring bloom and a second one later in the year.

Whereas α can be determined directly, β and χ in Eq. (6) will be estimated by minimisation. A realistic value for α is 0.9 g m^{-3} FTU^{-1}, the lowest ratio of SPM to Turbidity observed in winter (Fig. 7a and f).

β and χ have been estimated using the AMOEBA function of IDL (Interactive Data Language). This function performs multidimensional minimisation using the downhill simplex method. It has been applied to the minimisation of the mean square of the deviation between the logarithm of the observed SPM and SPM derived from Turbidity and Chlorophyll-*a* through Eq. (6). Using the logarithm of SPM gives a better representation of the low and medium levels (spring to autumn). 852 matchups of in situ Turbidity, SPM and Chlorophyll-*a* data have been used. χ is particularly difficult to estimate by minimisation, due to the small contribution of the phytoplankton biomass to total SPM and the strong variability of all the parameters in spring and summer, leading to low correlation between SPM and Turbidity during the productive season (Fig. 7 and Table 3). χ has been fixed

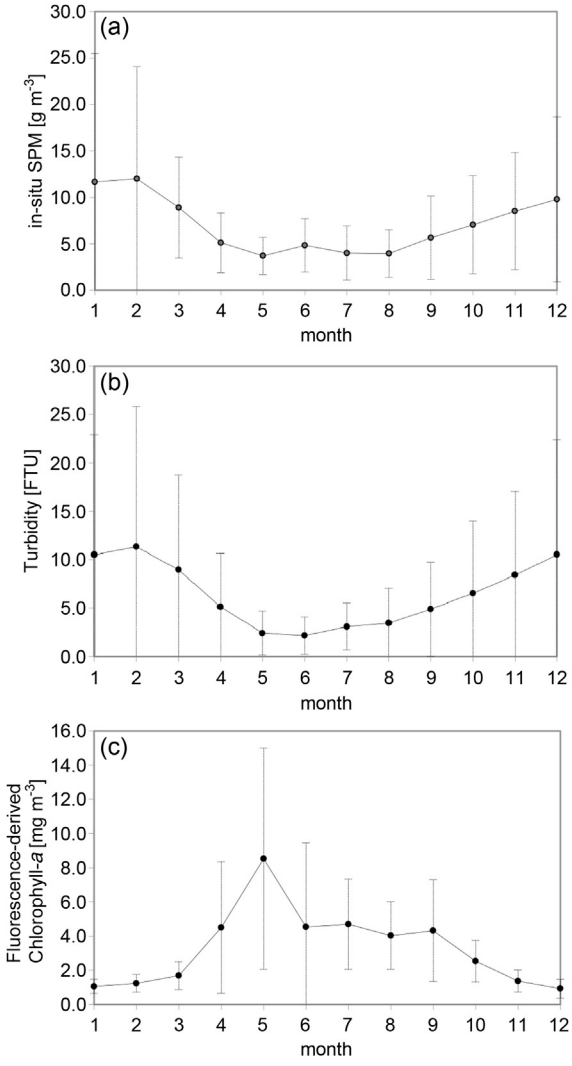

Figure 5 Monthly-averaged in situ observations at the mooring for the period 2003–2010: (a) SPM; (b) Turbidity; (c) fluorescence-derived chlorophyll-*a*. Bars indicate ± one standard deviation about the mean.

arbitrarily to 0.6, a level close to the mean summer Turbidity: SPM ratio. Another test has been made by adding a phase into the cosine term but without clear gain, as a zero phase corresponding to the first of January is well adapted to the winter maximum.

Finally, Eq. (7) expresses the relationship between SPM and Turbidity resulting from the minimisation.

$$\mathrm{SPM} = \left[0.9 + 0.48 \times \left(1 - \cos\left(\frac{\mathrm{time} \times 2\pi}{365}\right)\right)\right] \times [\mathrm{Turbidity} - 0.6 \times \mathrm{algal\ SPM}] + \mathrm{algal\ SPM}, \quad (7)$$

Table 2 Number of data available for each month during the 2003–2010 period.

Month	1	2	3	4	5	6	7	8	9	10	11	12	Total
In situ SPM	103	98	108	168	186	63	73	127	84	90	94	125	**1319**
Turbidity	11,905	10,848	11,695	10,973	8935	7852	7593	10,413	6509	9086	6059	8813	**110,681**
Fluorescence Chl	9086	7297	7411	6118	6785	3556	3943	6407	4319	5914	2349	5794	**68,979**
Satellite data	33	45	46	56	54	63	44	43	38	43	21	22	**508**

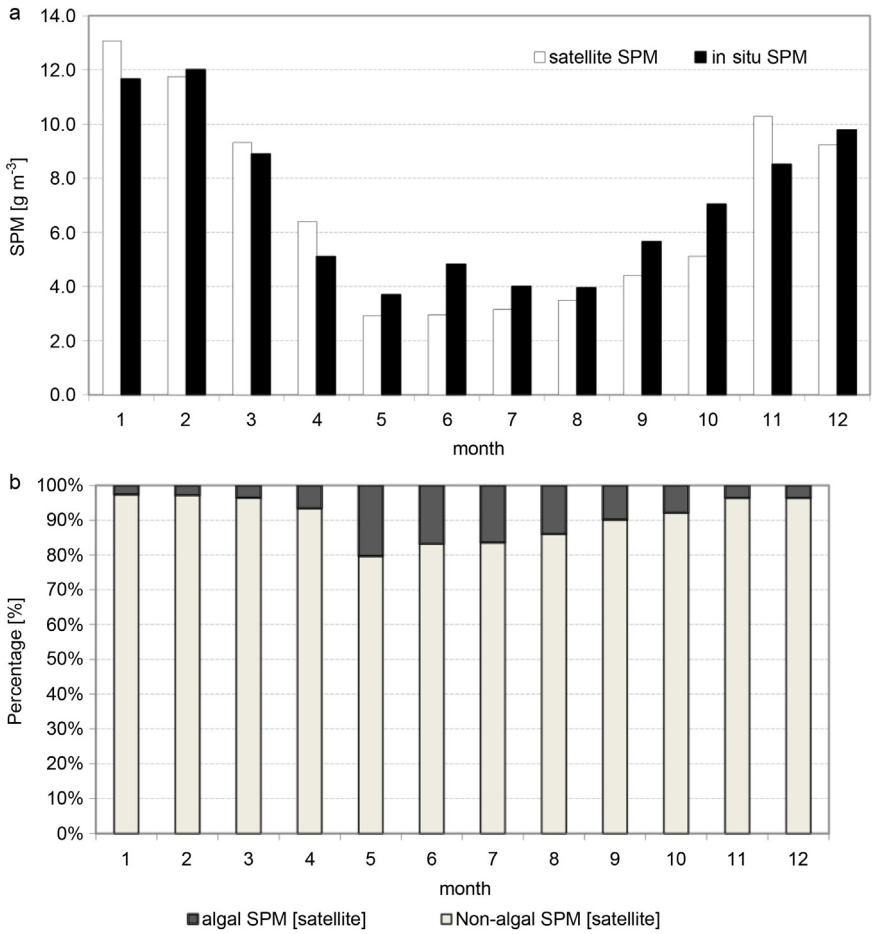

Figure 6 Monthly-averaged SPM for the period 2003–2010 and percentage of non-algal and algal components in the satellite-derived SPM: (a) Satellite and in situ SPM; (b) Percentage of non-algal and algal SPM in the satellite-derived SPM. Satellite and in situ SPM data considered for calculating the monthly averages of this graph have been observed at the same days.

for SPM and algal SPM in [g m^{-3}] and Turbidity in [FTU].

Fig. 8 shows Turbidity versus observed SPM with the 1:1 line superimposed. Points with high Turbidity (mostly in winter) tend to lie a little above the 1:1 line. Points with low Turbidity (mostly in summer) show a definite tendency to lie below the 1:1 line.

Fig. 9 shows observed SPM derived from Turbidity and Chl-*a*, after application of the seasonal modulation (equation 7), versus in situ SPM. The variability on the scatterplot shown in Fig. 9 around the line $Y = X$ is lower than using Turbidity as an estimator of SPM (as is the case in Fig. 8). The Mean Relative Error (MRE), related to the bias, $\Sigma(\mathbf{Y_i} - \mathbf{X_i})/\mathbf{X_i}$, and the Mean Relative Absolute Difference (MRAD), $\Sigma|\mathbf{Y_i} - \mathbf{X_i}|/\mathbf{X_i}$, are −0.21 and 0.37 respectively when SPM (X) is estimated by Turbidity (Y) (Fig. 8) and 0.07 and 0.40 when SPM (Y) is derived from the seasonally-modulated Turbidity and Chlorophyll-*a* (Fig. 9).

The gain in accuracy by applying a modulation to the Turbidity for estimating SPM is significant in the mean relative error. There is a reduction in the MRE (−0.21 to 0.07) but a slight increase in the MRAD (0.37–0.4), despite the significant reduction in the difference of the logarithms obtained through the minimisation. The seasonal modulation helps to correct the summer bias but not the strong variability (noise) already observed in the SPM:Turbidity relationship from May to August in Fig. 7.

3.3. Relationship between satellite-derived b_p and Turbidity at the mooring

In the semi-analytical algorithm, a switch is performed between b_b derived from the green and red wavelengths depending on the estimated SPM level. For low SPM levels (less than 4 g m^{-3}) the "green" SPM is chosen whereas for high SPM it is the "red" SPM. At the mooring the "green" b_b is often selected in summer, from May to July, and the "red" b_b in the other months. Fig. 10 shows the histogram of the selected wavelength throughout the seasons.

Fig. 11 shows the respective parts of the backscattering originating from non-algal particles and phytoplankton following formula (3). Even in summer, the mineral contribution is dominant in the total backscattering. The maximum phytoplankton contribution is observed in May when there is a peak in Chlorophyll-*a* and a drop in NA_SPM. Fig. 12 shows a good correlation between the seasonal cycles of in situ Turbidity and satellite-derived total backscattering (here in the red).

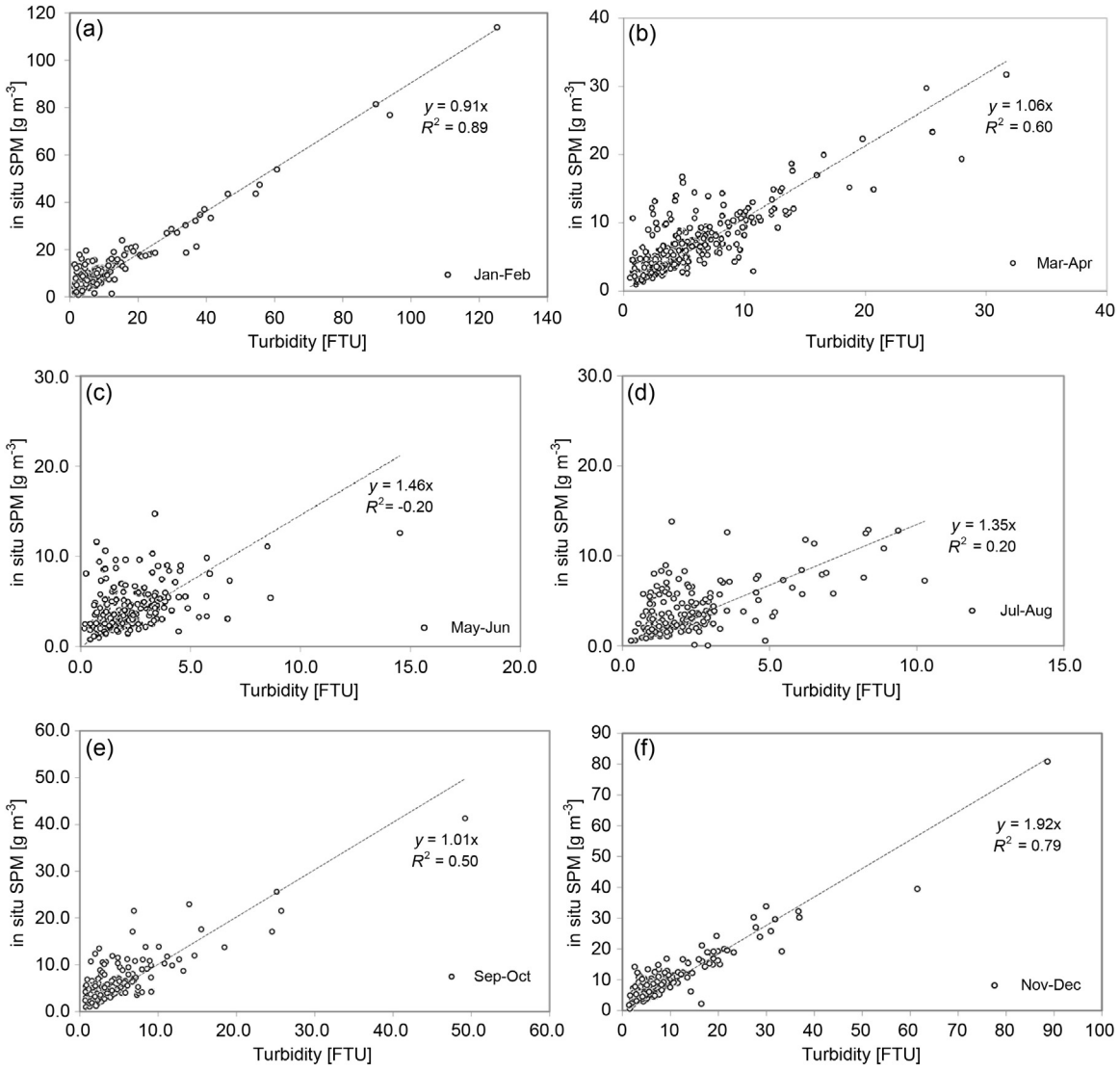

Figure 7 In situ SPM versus Turbidity for two-month periods.

Fig. 13 shows the scatterplot of the satellite-derived b_{bp} (non-algal and algal) versus Turbidity. The match-ups between Turbidity and satellite-derivedb_{bp} have been calculated for a time difference between satellite and in situ measurement of less than 30 min (499 matchups). The relationship is good but we observe relatively higher b_{bp} when Turbidity is low (from the green reflectance). The line $Y = 0.0082X$, corresponding to the regression of b_{bp} on Turbidity in the red wavelength, forced through the origin, is also indicated in Fig. 13. This line corresponds to a Turbidity-specific backscattering coefficient of 0.0082 m^{-1} FTU^{-1}.

Fig. 14 shows the scatterplot of the satellite-derived SPM versus the in situ SPM from daily match-ups. The time difference between the satellite and the in situ SPM may reach 13 h depending on the satellite orbit as most of the in situ data were sampled at midnight. When several samples

Table 3 SPM versus Turbidity for two-month periods. Average Turbidity, ratio of average SPM to average Turbidity, and parameters of the regression forced through the origin.

Month	Number of data	Average Turbidity [FTU]	Ratio SPM:Turbidity [g m^{-3} FTU^{-1}]	Equation	R^2
Jan–Feb	201	10.96	1.08	SPM = 0.91Turb	0.89
Mar–Apr	276	5.37	1.23	SPM = 1.06Turb	0.60
May–Jun	249	2.15	1.85	SPM = 1.46Turb	−0.20
Jul–Aug	200	2.49	1.59	SPM = 1.35Turb	0.20
Sep–Oct	174	4.78	1.33	SPM = 1.01Turb	0.50
Nov–Dec	219	8.29	1.11	SPM = 0.92Turb	0.79

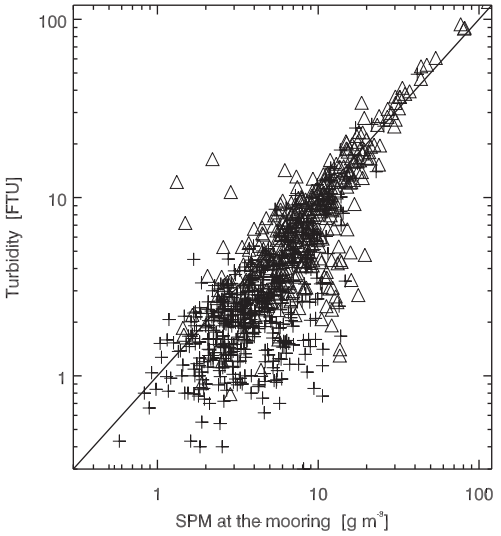

Figure 8 Turbidity versus in situ SPM. Crosses indicate "summer" data from April to October and triangles "winter" data from November to March. The correlation coefficient, calculated from 851 pairs of data, is equal to 0.94.

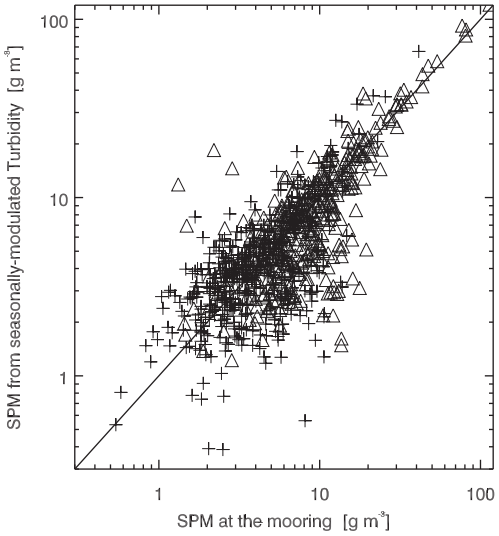

Figure 9 SPM derived from seasonally-modulated Turbidity and Chlorophyll-*a* versus in situ SPM. Crosses indicate "summer" data from April to October and triangles "winter" data from November to March. The correlation coefficient, calculated from 851 pairs of data, is equal to 0.92.

are made on the same day, the data are averaged to get one pair of measurements of SPM and Turbidity. 145 match-ups of satellite-derived SPM, in situ SPM and Turbidity are available from our data files. The MRE and MRAD are respectively 0.04 and 0.51 for satellite SPM compared to in situ SPM (Fig. 14) and 0.37 and 0.512 for satellite SPM compared to in situ Turbidity (Fig. 15).

We can make two comments from these graphs. The first is that the satellite-derived SPM is better related to in situ Turbidity (Fig. 15) than to in situ SPM (Fig. 14) if we do not consider the bias. This can be explained by the fact that the Turbidity is an optical parameter related to the backscattering as is the satellite SPM. Turbidity is also less subject to measurement error than in situ SPM. The second comment concerns the good estimation of SPM from the red reflectance and the under-estimation from the green reflectance (Fig. 14). A part of the seasonality is taken into account through the switch activated in the satellite algorithm but it is not sufficient. The red reflectance is chosen when the retrieved SPM is relatively high (4 g m^{-3}); which should have favoured a calibration of this part of the algorithm in the red from winter match-ups in coastal waters. Conversely, the calibration of the algorithm in the green would have been partly carried out in summer but not enough to counterbalance the jump in the SPM:Turbidity ratio in summer. Fig. 14 confirms the underestimation of the summer SPM (at low in situ SPM) by the satellite processing already observed in the mean seasonal comparisons shown in Fig. 6.

Table 4 gives a summary on the correlations and coefficients of the regression (intercept and slope) between the investigated variables. We observe from this table a better correlation between satellite SPM and Turbidity than between satellite SPM and in situ SPM. We observe also that the red b_b is better related to Turbidity than the green b_b. This is likely due to the variability of the particles in summer when b_b green is selected by the switching algorithm.

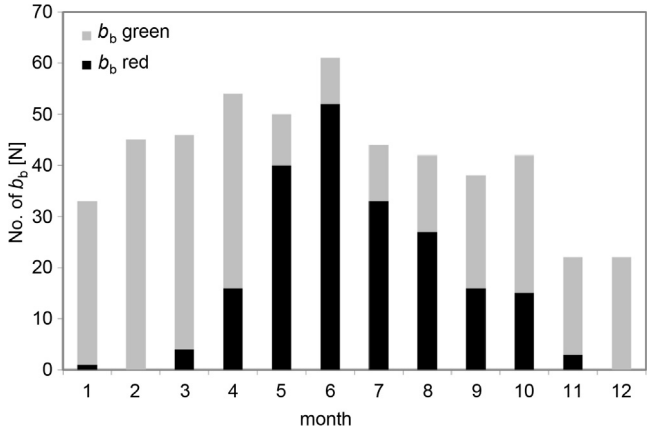

Figure 10 Number of satellite-derived b_{bred} and b_{bgreen} during the period 2003–2010. By construction the algorithm switches from b_{bred} to b_{bgreen} in the case of low Turbidity as observed in spring and summer.

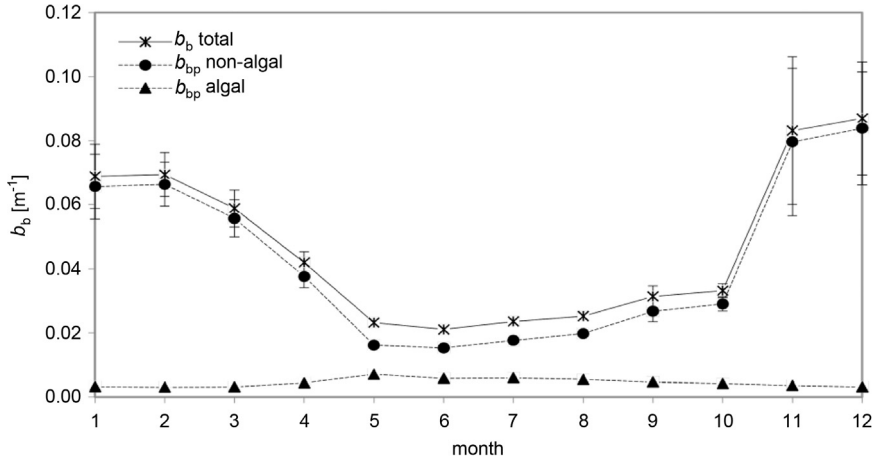

Figure 11 The seasonal cycle of the satellite-derived particle backscattering coefficient b_{bp} attributed to non-algal (NA_SPM) and algal (Chl) particles in the red wavelength (667 nm) at the mooring for the period 2003—2010.

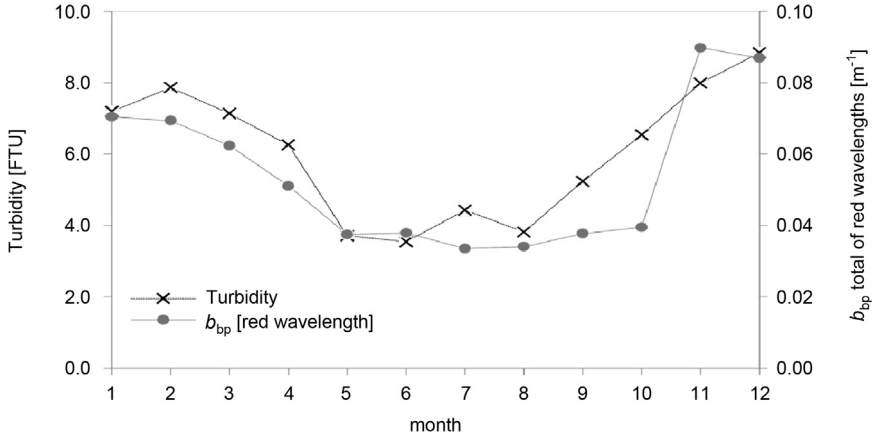

Figure 12 Mean seasonal cycles of the Turbidity and of the backscattering coefficient of particles (non-algal and algal) in the red wavelength (667 nm).

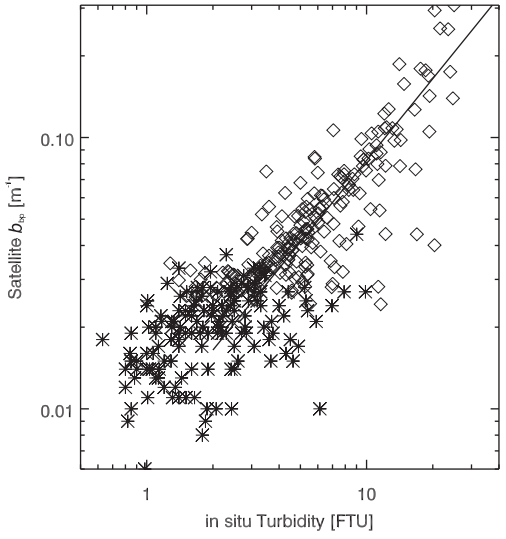

Figure 13 Backscattering of particles (non-algal and algal) versus Turbidity. Diamonds indicate an origin from red wavelength and stars from green wavelength. Line $Y = 0.0082X$ is indicated on the graph.

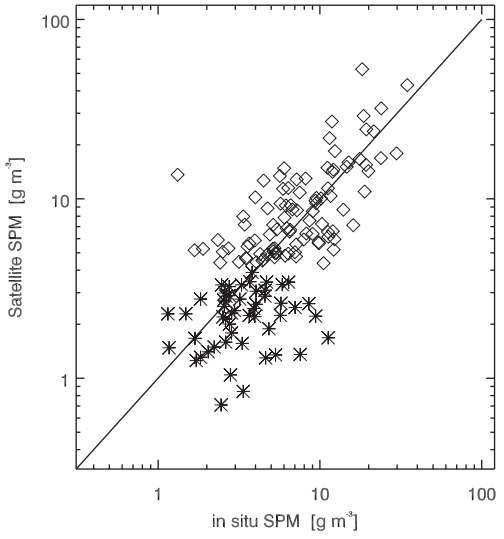

Figure 14 Satellite-derived SPM versus in situ SPM. Diamonds indicate an origin from red wavelength and stars from green wavelength. The correlation coefficient, calculated from 145 pairs of data, is equal to 0.74.

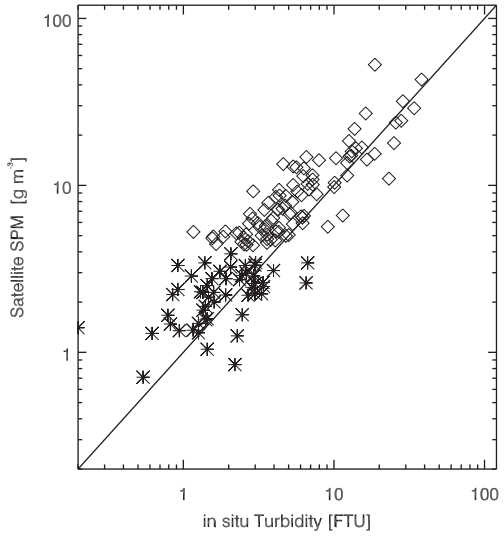

Figure 15 Satellite-derived SPM versus in situ Turbidity. Diamonds indicate an origin from red wavelength and stars from green wavelength. The correlation coefficient, calculated from 145 pairs of data, is equal to 0.86.

From this exceptional data set of in situ data we have observed a clear seasonal variation of the relationship between SPM and Turbidity, which was expected as the nature of the particles is known to vary with the season in this region. This relationship has been formalised through an equation with a seasonal modulation of the SPM:Turbidity ratio varying sinusoidally through the year.

The turbidity units of FTU are analogous to a backscattering coefficient and so the seasonal variation in the SPM:Turbidity ratio observed at the mooring is consistent with a seasonal variation in the mass-specific backscattering coefficient of particles, b_{bp}^*, with high values of b_{bp}^* in winter and low values in summer. It is therefore reasonable to expect that the seasonal variations in the SPM:Turbidity ratio are also associated with changes in the mass-specific backscattering coefficient of particles whose size, density and refractive index evolve through the seasons. Since SPM derived from the satellite algorithm depends on the value of b_{bnap}^* (which is assumed to be constant), this seasonal variation of b_{bnap}^* produces an under-estimate of SPM concentrations in the summer, but correct values of the SPM in the winter.

By construction, the satellite algorithm uses b_{bnap} in the green wavelength for inferring NA_SPM in low turbidity waters, in practice in summer, whereas it is b_{bnap} in the red that is mostly considered in winter. However, the rationale behind the application of a switch between the wavelengths in the satellite algorithm was not to take into account the different natures of particles through the seasons. The algorithm was initially calibrated using a data set of observations gathered through cruises in oceanic waters where the signal in the red wavelength was low (Gohin et al., 2005). SPM concentration was low to moderate and the selection of the green channel, with its ability to penetrate deeper into the water column, was appropriate. When coastal data, including very turbid waters, were monitored, the necessity to switch to the red wavelength became clear (Gohin, 2011). The unexpected effect of this switch is to have partly adapted the method to seasonal changes in particle type, which is particularly appropriate at the Liverpool station where 4 g m^{-3}, the switch threshold, is close to the summer level of SPM. Both calibrations being almost independent (only the consistency of the evaluations at about 4 g m^{-3} is checked), a part of the variability between a low backscattering coefficient of non-algal particles in summer and a higher value in winter was achieved through the estimation of the two pairs of parameters α_0 and α_1 in Eq. (1) for the green and red wavelengths. This can explain partly the robustness of the satellite algorithm. These results corroborate what has been observed at the coastal stations of the Ifremer phytoplankton REPHY network, from the North-Sea to the Mediterranean Sea, by Gohin (2011). A large time series of Turbidity measurements (ranging from 2003 to 2009) was analysed in the 2011 study. A distinction was made between the data of the old turbidimeters expressed in NTU (Nephelometric Turbidity Unit) units and those of the new generation of instruments and methods in FTU. Despite the better adaptation of the recent instruments for measuring the particle content obtained through an Infra-red wavelength at 860 nm, the satellite-based climatology of Turbidity was calculated from the measurements in [NTU] that were the most numerous in the REPHY data base; the FTU data starting to be collected only in 2008. In the 2011 study, Turbidity in [FTU] was observed to be superior to Turbidity in NTU by a factor 1.27 and Turbidity in [NTU] was expressed as 0.54 SPM [g m^{-3}]; which gives Turbidity in [FTU] equal to 0.69 SPM. Despite numerous approximations in this study based on the historical Turbidity measurements available from the Ifremer REPHY network, the relationship between satellite-derived and observed Turbidity data was better than for chlorophyll *a*nd the factor of 0.69 for the SPM:Turbidity ratio is in agreement with what has been observed at the

Table 4 Correlation coefficient, intercept at the origin and slope of the regression between variables.

Variables	Time difference	Coefficient of correlation	Intercept	Slope	Number of data
In situ SPM and Turbidity	<20 nm	0.94	−1.9	1.07	851
In situ SPM and SPM derived from Turbidity and Chl by applying the seasonal modulation	<20 nm	0.92	−0.4	1.04	851
Sat SPM and in situ SPM	Same day	0.75	3.18	0.57	145
Sat SPM and in situ Turbidity (when SPM is available)	Same day	0.86	0.54	0.74	145
Sat b_{bp} (green) and in situ Turbidity	<20 nm	0.41	0 (forced)	0.0066	150
Sat b_{bp} (red) and in situ Turbidity	<20 nm	0.83	0 (forced)	0.0082	222

Liverpool Bay station. Focusing on Turbidity, and not non-algal SPM, Turbidity could be estimated directly from satellite-derived b_{bp} by using the relationship shown in Fig. 13:

$$b_{bp}[m^{-1}] = 0.0082\,\text{Turbidity}\,[\text{FTU}].$$

4. Conclusion

At the location of the mooring in the Irish Sea, over an 8-year period, we found results similar to those of Dogliotti et al. (2015) showing, at different coastal sites, that Turbidity is a key parameter to be estimated from marine reflectance. The semi-analytical methods in the red wavelength perform relatively well in low to medium Turbidity and Turbidity is retrieved with better success than SPM. The satellite-derived backscattering coefficient and the Turbidity are two optical properties that are tightly related. We have seen that applying a seasonal modulation to the in situ Turbidity improves the estimation of SPM by diminishing the summer bias. Despite this clear seasonal variation of the particle type and size that could affects the retrieving of SPM from satellite data processed by semi-analytical algorithms throughout the year, the switch operated in the satellite algorithm limits this effect at the location of the Liverpool Bay mooring. As shown in Han et al. (2016) this algorithm provides relatively good retrievals for a large variety of coastal waters where SPM [g m^{-3}] ranges within the limits [0,50]. We also know that in some places where the neap/spring cycle of Turbidity has been observed from space (Shi et al., 2011; Rivier et al., 2012), the nature of the particles may change following the lunar cycle with bigger aggregates, therefore probably lower b_{bnap}^{*}, at neap tides. In other areas, like the continental shelf of the Bay of Biscay where the impact of the tidal cycle is relatively low, a seasonal modification of the satellite algorithm could be proposed, with mass-specific backscattering coefficients in the green and the red different for the windy winter season and the summer (Gohin et al., 2015). b_{bnap}^{*} could be also determined partially from the intensity of the waves, particularly in winter, whereas the spring to autumn variability of b_{bnap}^{*} induced by the biology could be improved by a better knowledge of the TEPs (Transparent Exopolymer Particles). Improving our knowledge on the TEPs is a common issue to remote-sensing and modelling of SPM (Van der Molen et al., 2009). The contribution of the phytoplankton to the IOPs and to the algal biomass could be also improved by using local information on phytoplankton groups (observations or outputs of ecological models). We can also mention the very specific signal of detached coccoliths, often visible on SPM images in the North Atlantic, whose reflectance should be analysed separately (Moore et al., 2012; Smyth et al., 2002).

In conclusion, Turbidity is probably the key parameter to be estimated from space but as Turbidity measurements have been generally carried out in order to be transformed into SPM using local calibrations, little attention has been paid to the Turbidity values themselves and the variability of the turbidimeters is large in term of wavelengths and scattering angles of observation. Remote-sensing is a good tool for helping final users and turbidimeter builders to progress in cooperation for defining instruments and calibration methods better adapted to the monitoring of large coastal areas.

Acknowledgments

The authors are grateful to the Ocean Biology Distributed Active Archive Center at NASA, Greenbelt, MD, USA, for the provision of MODIS-Aqua data. We are also grateful to the Liverpool Bay Coastal Observatory, National Oceanographic Centre, UK for providing the SmartBuoy mooring data in the Liverpool Bay and NERC/DEFRA for funding the SmartBuoy and monitoring program. This work was carried out under Ministry of Higher Education (MOHE) Malaysia scholarship with collaboration with Universiti Malaysia Sabah (UMS). It also contributes to the validation of the non-algal SPM products provided for the Atlantic North-West Shelf by the Ocean Colour TAC of the Copernicus Marine Environment Monitoring Service.

References

Berthon, J.F., Shybanov, E., Lee, M.E., Zibordi, G., 2007. Measurements and modeling of the volume scattering function in the coastal northern Adriatic Sea. Appl. Opt. 46 (22), 5189–5203, http://dx.doi.org/10.1364/AO.46.005189.

Binding, C.E., Bowers, D.G., Mitchelson-Jacob, E.G., 2003. An algorithm for the retrieval of suspended sediment concentrations in the Irish Sea from SeaWiFS ocean colour satellite imagery. Int. J. Remote Sens. 24 (19), 3791–3806, http://dx.doi.org/10.1080/0143116021000024131.

Bowers, D.G., Hill, P.S., Braithwaite, K.M., 2014. The effect of particulate organic content on the remote sensing of marine suspended sediments. Remote Sens. Environ. 144, 172–178, http://dx.doi.org/10.1016/j.rse.2014.01.005.

Devlin, M.J., Barry, J., Mills, D.K., Gowen, J., Foden, J., Sivyer, D., Greenwood, N., Pearce, D., Tett, P., 2009. Estimating the diffuse attenuation coefficient from optically active constituents in UK marine waters. Estuar. Coast. Shelf Sci. 82 (1), 73–83, http://dx.doi.org/10.1016/j.ecss.2008.12.015.

Dogliotti, A.I., Ruddick, K.G., Nechad, B., Doxaran, D., Knaeps, E., 2015. A single algorithm to retrieve Turbidity from remotely sensed data in all coastal and estuarine waters. Remote Sens. Environ. 156, 157–168, http://dx.doi.org/10.1016/j.rse.2014.09.020.

Edwards, K.P., Barciela, R., Butenschön, M., 2012. Validation of the NEMO-ERSEM operational ecosystem model for the North West European Continental Shelf. Ocean Sci. 8 (6), 983–1000, http://dx.doi.org/10.5194/os-8-983-2012.

Eleveld, M.A., Pasterkamp, R., Van der Woerd, H.J., Pietrzak, J., 2008. Remotely sensed seasonality in the spatial distribution of sea-surface suspended particulate matter in the southern North Sea. Estuar. Coast. Shelf Sci. 80 (1), 103–113, http://dx.doi.org/10.1016/j.ecss.2008.07.015.

Ford, D.A., van der Molen, J., Hyder, K., Bacon, J., Barciela, R., Creach, V., McEwan, R., Ruardij, P., Forster, R., 2017. Observing and modelling phytoplankton community structure in the North Sea. Biogeosciences 14 (6), 1419–1444, http://dx.doi.org/10.5194/bg-14-1419-2017.

Forget, P., Ouillon, S., Lahet, F., Broche, P., 1999. Inversion of reflectance spectra of non-chlorophyllous turbid coastal waters. Remote Sens. Environ. 68 (3), 264–272, http://dx.doi.org/10.1016/S0034-4257(98)00117-5.

Gohin, F., 2011. Annual cycles of chlorophyll-*a*, non-algal suspended particulate matter, and Turbidity observed from space and in situ in coastal waters. Ocean Sci. 7 (5), 705–732, http://dx.doi.org/10.5194/os-7-705-2011.

Gohin, F., Druon, J.N., Lampert, L., 2002. A five channel chlorophyll concentration algorithm applied to SeaWiFS data processed by

Seadas in coastal waters. Int. J. Remote Sens. 23 (8), 1639–1661, http://dx.doi.org/10.1080/01431160110071879.

Gohin, F., Loyer, S., Lunven, M., Labry, C., Froidefond, J.M., Delmas, D., Huret, M., Herbland, A., 2005. Satellite-derived parameters for biological modeling in coastal waters: illustration over the eastern continental shelf of the bay of Biscay. Remote Sens. Environ. 95 (1), 29–46, http://dx.doi.org/10.1016/j.rse.2004.11.007.

Gohin, F., Bryère, P., Griffiths, J.W., 2015. The exceptional surface Turbidity of the North-West European shelf seas during the stormy 2013–2014 winter: consequences for the initiation of the phytoplankton blooms? J. Mar. Syst. 148, 70–85, http://dx.doi.org/10.1016/j.jmarsys.2015.02.001.

Guillou, N., Rivier, A., Gohin, F., Chapalain, G., 2015. Modeling near-surface suspended sediment concentration in the English channel. J. Mar. Sci. Eng. 3 (2), 193–215, http://dx.doi.org/10.3390/jmse3020193.

Guillou, N., Rivier, A., Chapalain, G., Gohin, F., 2016. The impact of tides and waves on near-surface suspended sediment concentrations in the English Channel. Oceanologia 59 (1), 28–36, http://dx.doi.org/10.1016/j.oceano.2016.06.002.

Han, B., Loisel, H., Vantrepotte, V., Mériaux, X., Bryère, P., Ouillon, S., Dessailly, D., Xing, Q., Zhu, J., 2016. Development of a semi-analytical algorithm for the retrieval of Suspended Particulate Matter from remote sensing over clear to very turbid waters. Remote Sens. 8 (3), 211, http://dx.doi.org/10.3390/rs8030211.

Huret, M., Gohin, F., Delmas, D., Lunven, M., Garçon, V., 2007. Use of SeaWiFS data for light availability and parameter estimation of a phytoplankton production model of the Bay of Biscay. J. Mar. Syst. 65 (1–4), 509–531, http://dx.doi.org/10.1016/j.jmarsys.2005.07.007.

Lahet, F., Ouillon, S., Forget, P., 2000. A three-component model of ocean color and its application in the Ebro river mouth area. Remote Sens. Environ. 72 (2), 181–190, http://dx.doi.org/10.1016/S0034-4257(99)00101-7.

Li, Y., Huang, W., Fang, M., 1998. An algorithm for the retrieval of suspended sediment in coastal waters of China from AVHRR data. Cont. Shelf Res. 18 (5), 487–500, http://dx.doi.org/10.1016/S0278-4343(97)00074-5.

Loring, D.H., Rantala, R.T.T., 1992. Manual for the geochemical analyses of marine sediments and suspended particulate matter. Earth-Sci. Rev. 32 (4), 235–283, http://dx.doi.org/10.1016/0012-8252(92)90001-A.

Martinez-Vicente, V., Land, P.E., Tilstone, G.H., Widdicombe, C., Fishwick, J.R., 2010. Particulate scattering and backscattering related to water constituents and seasonal changes in the Western English Channel. J. Plankton Res. 32 (5), 603–619, http://dx.doi.org/10.1093/plankt/fbq013.

McKee, D., Cunningham, A., 2006. Identification and characterisation of two optical water types in the Irish Sea from in situ inherent optical properties and seawater constituents. Estuar. Coast. Shelf Sci. 68 (1–2), 305–316, http://dx.doi.org/10.1016/j.ecss.2006.02.010.

Ménésguen, A., Gohin, F., 2006. Observation and modelling of natural retention structures in the English Channel. J. Mar. Syst. 63 (3–4), 244–256, http://dx.doi.org/10.1016/j.jmarsys.2006.05.004.

Mills, D.K., Greenwood, N., Kröger, S., Devlin, M., Sivyer, D.B., Pearce, D., Cutchey, S., Malcolm, S.J., 2005. New approaches to improve the detection of eutrophication in UK coastal waters. Environ. Res. Eng. Manage. 2 (32), 36–42.

Moore, T.S., Dowell, M.D., Franz, B.A., 2012. Detection of coccolithophore blooms in ocean color satellite imagery: a generalised approach for use with multiple sensors. Remote Sens. Environ. 117, 249–263, http://dx.doi.org/10.1016/j.rse.2011.10.001.

Morel, A., 1988. Optical modelling of the upper ocean in relation to its biogeneous matter content (Case 1 water). J. Geophys. Res. 93 (C9), 10749–10768, http://dx.doi.org/10.1029/JC093iC09p10749.

Nechad, B., Ruddick, K., Park, Y., 2010. Calibration and validation of a generic multisensor algorithm for mapping of total suspended matter in turbid waters. Remote Sens. Environ. 114 (4), 854–866, http://dx.doi.org/10.1016/j.rse.2009.11.022.

Neil, C., Cunningham, A., McKee, D., 2011. Relationships between suspended mineral concentrations and red-waveband reflectances in moderately turbid shelf seas. Remote Sens. Environ. 115 (12), 3719–3730, http://dx.doi.org/10.1016/j.rse.2011.09.010.

Neukermans, G., Loisel, H., Mériaux, X., Astoreca, R., McKee, D., 2012. In situ variability of mass-specific beam attenuation and backscattering of marine particles with respect to particle size, density, and composition. Limnol. Oceanogr. 57 (1), 124–144.

Reynolds, R.A., Stramski, D., Neukermans, G., 2016. Optical backscattering by particles in Arctic seawater and relationships to particle mass concentration, size distribution, and bulk composition. Limnol. Oceanogr. 61 (5), 1869–1890, http://dx.doi.org/10.1002/lno.10341.

Rivier, A., Gohin, F., Bryère, P., Petus, C., Guillou, N., Chapalain, G., 2012. Observed vs. predicted variability in non-algal suspended particulate matter concentration in the English Channel in relation to tides and waves. Geo-Mar. Lett. 32 (2), 139–151, http://dx.doi.org/10.1007/s00367-011-0271.

Sharples, J., Simpson, J.H., 1995. Semi-diurnal and longer period stability cycles in the Liverpool Bay Region of Freshwater Influence. Cont. Shelf Res. 15 (2–3), 295–313, http://dx.doi.org/10.1016/0278-4343(94)E0003-5.

Shi, W., Wang, M., Jiang, L., 2011. Spring-neap tidal effects on satellite ocean color observations in the Bohai Sea, Yellow Sea, and East China Sea. J. Geophys. Res. Oceans 116 (C12), C12032, 13 pp., http://dx.doi.org/10.1029/2011JC007234.

Smyth, T.J., Moore, G.F., Groom, S.B., Land, P.E., Tyrrell, T., 2002. Optical modeling and measurements of a coccolithophore bloom. Appl. Opt. 41 (36), 7679–7688, http://dx.doi.org/10.1364/ao.41.007679.

Snyder, W.A., Arnone, R.A., Davis, C.O., Goode, W., Gould, R.W., Ladner, S., Lamela, G., Rhea, W.J., Stavn, R., Sydor, M., Weidemann, A., 2008. Optical scattering and backscattering by organic and inorganic particulates in U.S. coastal waters. Appl. Opt. 47 (5), 666–677, http://dx.doi.org/10.1364/AO.47.000666.

Sykes, P.A., Barciela, R.M., 2012. Assessment and development of a sediment model within an operational system. J. Geophys. Res. 117 (C4), C04036, 17 pp., http://dx.doi.org/10.1029/2011JC007420.

Tett, P.B., 1987. Plankton. In: Baker, J.M., Wolff, W.J. (Eds.), Biological Surveys of Estuaries and Coasts. Cambridge Univ. Press, Cambridge, 280–341.

Tilstone, G., Mallor-Hoya, S., Gohin, F., Belo Couto, A., Sa, C., Goela, P., Cristina, S., Airs, R., Icely, J., Zühlke, M., Groom, S., 2017. Which Ocean colour algorithm for MERIS in North West European waters? Remote Sens. Environ. 189, 132–151, http://dx.doi.org/10.1016/j.rse.2016.11.012.

Van der Molen, J., Bolding, K., Greenwood, N., Mills, D.K., 2009. A 1-D vertical multiple grain size model of suspended particulate matter in combined currents and waves in shelf seas. J. Geophys. Res. 114 (F1), F01030, 15 pp., http://dx.doi.org/10.1029/2008JF001150.

Van der Molen, J., Ruardij, P., Greenwood, N., 2016. Potential environmental impact of tidal energy extraction in the Pentland Firth at large spatial scales: results of a biogeochemical model. Biogeosciences 13 (8), 2593–2609, http://dx.doi.org/10.5194/bg-13-2593-2016.

Van der Molen, J., Ruardij, P., Greenwood, N., 2017. A 3D SPM model for biogeochemical modelling, with application to the northwest European continental shelf. J. Sea Res., http://dx.doi.org/10.1016/j.seares.2016.12.003 (in press).

Van der Woerd, H.J., Pasterkamp, R., 2008. HYDROPT: a fast and flexible method to retrieve chlorophyll-*a* from multispectral satellite observations of optically complex coastal waters. Remote Sens. Environ. 112 (4), 1795–1807, http://dx.doi.org/10.1016/j.rse.2007.09.001.

Wolf, J., Brown, J.M., Howarth, M.J., 2011. The wave climate of Liverpool Bay – observations and modelling. Ocean Dynam. 61 (5), 639–655, http://dx.doi.org/10.1007/s10236-011-0376-9.

Woźniak, S.B., 2014. Simple statistical formulas for estimating biogeochemical properties of suspended particulate matter in the southern Baltic Sea potentially useful for optical remote sensing applications. Oceanologia 56 (1), 7–39, http://dx.doi.org/10.5697/oc.56-1.007.